Eurographics Workshop on Urban Data Modelling and Visualisation (2016)
F. Biljecki and V. Tourre (Editors)

Optimizing Window Shape for Daylighting: An Urban Context Approach

E. Fernández [1†], J.P. Aguerre [1], B. Beckers [2] and G. Besuievsky [3]

[1] Centro de Cálculo, Universidad de la República, Uruguay
[2] Université de Pau et des Pays de l'Adour, France
[3] ViRVIG, Universitat de Girona, Spain

Abstract

Configuring the optimal shape and position of a building opening, such as windows or skylights, is a crucial task for daylight availability. Computing daylighting requires the use of climate-based data, which involves large data sets and a time-consuming task performed by procedures that in general are not well suited for optimization. In addition, optimal opening shapes may be strongly affected by the urban context, which is rarely taken into account or roughly approximated.

In this paper we present a new opening shape optimization technique that considers the urban environment. The exterior contribution is computed through a radiosity approximation. A pinhole-based model is used to model the influence of daylight component on the interior surfaces. Our results show the importance of the exterior influence in the final optimal shapes by computing the same room at different building locations.

1. Introduction

Daylighting plays a very important role for energy saving in sustainable building, and setting the optimal shapes and positions of the openings is crucial for improving the daylight availability. Optimizing the use of daylight concerns the use of climate-based data, and the hourly data-set for the whole year must be taken into account at each iteration of the optimization process. Concerning the daylight computation, we must evaluate the percentage in hours of daylight accessibility in a place, using any of the available metrics, like Daylight Autonomy (DA) [RMR06] or Useful Daylight Illuminance (UDI) [NM05]. Although consolidated methods are successfully used for interior studies, the exterior environment with the full action of its components is rarely addressed. Exterior obstructions and reflections, typically due to adjacent buildings and trees, may affect considerably the indoor daylight provided. Therefore, it is a very important parameter to consider in lighting simulation.

The problem of finding the optimal geometric model that achieves the goal of maximizing the daylight hours cannot be solved by standard CAD tools that work using forward-based strategies. Such strategies are unsuitable for optimization problems, where thousands of possible configurations should be tested. The problem should be stated as an inverse problem [FB12] and formulated with an optimization approach [CSFN11]. An additional difficulty is that we need to evaluate the whole hourly data-set of the year, at each iteration of the optimization process. Available daylight methodologies like the daylight coefficient approach [TW83] or the "three-phase simulation method" [WML*11, ML13] are not completely well suited for windows shape optimization. Recently, a fast methodology based on a pinhole approach has provided results that can achieve efficient opening shape optimization [FBB16]. However, the method does not take into account the exterior environment.

In this paper, we propose an opening shape optimization method that considers the urban context. That is, any exterior geometric model that can potentially obstruct or reflect light is integrated in the optimization procedure. The new method is based on the pinhole radiosity method [FB15, FBB16] and the sparsity of the form factor matrix in urban environments [AFBB16]. The proposal can deal with a whole-year data-set, providing fast daylighting computation for full global illumination solutions. Our test results show the different optimal window shape solution depending on the exterior environment. The results enhance the importance of computing all exterior components correctly for daylighting assessment.

2. Related Work

2.1. Daylighting Computation

One of the most used daylight metric is the UDI [NM05], which indicates the number of hours in the year when the illuminance values are above a desired minimum, typically 100lx, and below a desired maximum, typically 2000lx. Unlike other similar metrics,

[†] eduardof@fing.edu.uy

DOI: 10.2312/udmv.20161418

UDI captures the daylight sufficiency and visual comfort of a design solution because values above the upper threshold are likely to cause visual discomfort/glare. To compute the daylight performance of an interior space, the annual hourly illuminance values are calculated over some sensors representing a work plane, typically at 0.75m height. The total illuminance reaching a sensor can be split into three components: the sky component (SC), which is the direct light entering the room, the exterior reflected component (ERC), which is the incoming light arriving after reflection on other buildings, and the interior reflected component (IRC), which is the light reaching the sensor after internal reflections [Rei14]. Methods that take into account the exterior can consider SC by using masks, like the ones available in Autodesk Ecotect [Aut14], but the ERC is rarely used.

Regarding the daylighting computation, one of the most used methods is based on the Daylight Coefficient (DC) approach originally proposed by Tregenza [TW83]. The concept of DCs is to divide the sky dome into a set of sky tiles and then calculate the contribution of each sky tile to the total illuminance at various sensors. The sensors are characterized by their position and orientation, and their total illuminance is obtained by linear superposition of each DC. Working with DCs is a two-step process: first calculating the DCs, and then folding them against time-varying luminances. The approach is very efficient for static scenes, but, when the geometry changes, the DCs should be re-computed. This discourages the use of a DC approach for optimization problems. However, it is computationally possible with time consuming executions. Recent approaches [FOB15, HW15] follow this strategy, and aim to link daylighting to energy performance, without considering exterior obstructions.

2.2. Opening Optimization and Inverse Lighting Problems

Early approaches to inverse opening shape design can be found in [TMH08, BT09]. They consider openings composed of a set of small elements as in the present work, but time consuming results are obtained for simple cases without the correct use of global illumination. More optimal results exploit the use of coherence in architectural models using a low-rank radiosity (LRR) approach in combination with a meta-heuristic method for optimization [FB12, FB14]. However, these methods are restricted to translucent surfaces like diffuse skylights and they do not take into account annual climate-based data. More recently, a method based on a pinhole approach has provided results that can achieve efficient shape opening optimization [FB15, FBB16]. In [FB15], basic exterior obstructions are already taken into account, but they do not consider external reflections and they only consider static skies. On the other hand, the method provided in [FBB16] considers daylighting as lighting intention using climate-based data, but lacking of any exterior building incidence. This is the problem we tackle in the present paper.

3. A Urban Context approach

3.1. Overview of the method

Our method uses the Tregenza's 145 sky tile discretization [TW83]. Given a building localized in an urban model and an interior model, where openings should be installed, our method works following a pre-processing step and an optimization one. First, an approximated urban radiosity solution is obtained for each sky tile (Sec. 3.2). This solution is used in combination with climate-based data and processed with the pinhole illuminace method [FBB16], to obtain a compact representation that relates the interior sensors with the opening elements and the sky dome (Sec. 3.3). Finally, an optimization process aiming to maximize the UDI is executed to compute the final shapes (Sec. 3.4).

3.2. Computing the exterior

The illumination of the city environment is computed using the radiosity algorithm over the selected urban model. The radiosity algorithm [CWH93] is a technique that approximates global illumination using a finite element methodology. The scene is discretized into n_c elements, also called patches, leading to a set of linear equations. Eq. 1 expresses these equations in a succinct manner.

$$(\mathbf{I}_c - \mathbf{R}_c\mathbf{F}_c)B_c = E_c, \tag{1}$$

Here, $\mathbf{I}_c$ is the identity matrix, $\mathbf{R}_c$ is a diagonal matrix containing the reflectivity index of each patch, B_c is the radiosity vector to be found (W/m^2), and E_c is the emission vector. $\mathbf{F}_c(i,j)$ is a number between 0 and 1 expressing the form factor between patch i and j. This value indicates the fraction of the light power going from one to another. Therefore, the form factor matrix is a $n_c \times n_c$ matrix.

Once $\mathbf{F}_c$ is computed, the radiosity vector B_c corresponding to a particular emission configuration (E_c) can be calculated by solving the linear system iteratively. Eq. 2 shows the radiosity step using the Jacobi iteration methodology.

$$B_c^{(i+1)} = \mathbf{R}_c\mathbf{F}_c B_c^{(i)} + E_c \ , \ \text{where } B_c^{(0)} = E_c \tag{2}$$

Each iteration adds the radiosity of a new light bounce to the global radiosity result. This process is repeated until $||B_c^{(i+1)} - B_c^{(i)}||$ is less than an expected error threshold.

Following [AFBB16], the memory requirements associated with the form factors matrix of a city model can be significantly reduced using sparse representations. This is explained by the high occlusion factor present in urban environments, where a patch i is commonly not seen by most patches j (which means that $\mathbf{F}_c(i,j) = 0$). Typically only 1% of $\mathbf{F}_c$ components are nonzero. This fact allows to work with big models using a small storage capacity, and accelerates the computation of matrix-vector and matrix-matrix products.

Since the only emitters are the sky tiles (145 elements), a pre-computation step is executed to speed-up the process. A set of 145 radiosity results are computed using the Jacobi iteration for 145 E_c vectors, where each configuration corresponds to each sky tile emitting only by itself (a vector with all zeros except for a 1 in the patch index). Because the contribution of each sky tile to the city is independent, the radiosity result corresponding to a sky emission configuration can be computed by a linear combination of the previous 145 B_c vectors, which is a simple operation that can be performed quickly. Therefore, after this pre-computation process, many thousand sky configurations can be solved in very short execution times.

3.3. Fast Daylighting Computation

In this section, we explain the calculation of the illuminance at the interior of any geometric model where daylight comes through an opening, as it happens in an office. We used a pinhole based method (PBM) [FB15, FBB16] (see Fig. 1) which allows to model anisotropic emissions and isotropic reflections. This method consists in replacing an opening by a set of pinholes. In turn, each pinhole j is modeled by the use of two opposite hemi-cubes, $\mathbf{H}_j^E$ and $\mathbf{H}_j^I$. These hemi-cubes allow to link the inner scene patches with the exterior light coming through the pinhole.

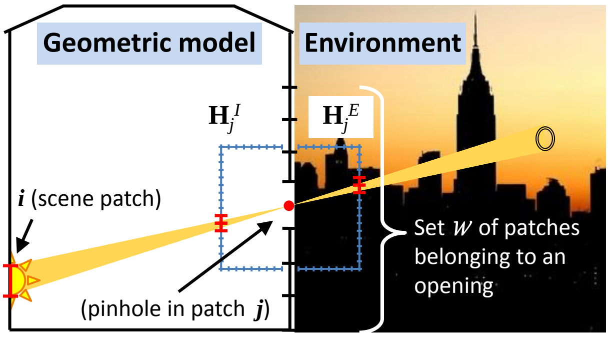

Figure 1: *Pinhole based method and its components [FBB16].*

The illuminance equation used (Eq. 3) is a variant of Eq. 1. It is used to calculate the luminous flux (I) incident on all patches of the interior geometry:

$$(\mathbf{I}_o - \mathbf{F}_o\mathbf{R}_o)I = \mathbf{F}_o E_o + \mathbf{G}_s W \tag{3}$$

Besides containing $\mathbf{I}_o$, $\mathbf{F}_o$, $\mathbf{R}_0$ of dimension $n_o \times n_o$ (n_o is the number of interior patches) and E_o, the equation includes the matrix $\mathbf{G}_s$ of dimension $n_o \times \bar{w}$ ($\bar{w}$ is the number of pinholes), and a vector W used to define the opening. The vector $\mathbf{G}_s W$ determines the direct illuminance of daylight on the inner geometry, which is used in Eq. 3 as source of light. $\mathbf{G}_s(i,j)$ contains the direct illuminance at patch i coming from the exterior environment through pinhole j. By definition, $\mathbf{G}_s$ depends on the sky configuration s. W is a binary vector, where $W(j)=1$ when the patch j is open, and $W(j)=0$ otherwise.

In this work, luminaries and other light sources different from daylight are ignored, resulting in $E=0$. After this simplification, Eq. 3 is transformed into Eq. 4 to speed up the calculation of I.

$$I = \mathbf{N}_s W, \quad \text{where } \mathbf{N}_s = (\mathbf{I}_o - \mathbf{F}_o\mathbf{R}_o)^{-1}\mathbf{G}_s \tag{4}$$

For small scenes, the inverse of $(\mathbf{I}_o - \mathbf{F}_o\mathbf{R}_o)$ can be calculated directly (with a complexity of $O(n_o^3)$ and $O(n_o^2)$ memory) using nowadays personal computers. For medium to large scenes with spatial coherence, the inverse matrix can be approximated using the LRR method (with complexity $O(n_o k^2)$ and memory $O(n_o k)$, where $k \ll n$ [FB12]) or other factorization techniques. An important property of Eq. 4 is that it is possible to calculate the illuminance of any subset of patches directly, as for example a set P defined as sensors, without the previous calculation of the illuminance in the entire scene. This is because $I(P)=\mathbf{N}_s(P,:)W$. Then, $I(P)$ requires only $O(\bar{P}\bar{w})$ operations and memory. Of course, the simplification is useful only for static geometry. The rest of the section is devoted to factorize $\mathbf{N}_s$ into a sky invariant component ($\mathbf{Q}$) and the sky configuration (s).

The calculation of $\mathbf{G}_s$ is expressed in Eq. 5. In this equation, $\mathbf{H}_j^E$ and $\mathbf{H}_j^I$ are hemi-cubes with the external and internal views of the scene, respectively (see Figs 1, 2(a) and (e)), $\Delta\mathbf{F}$ contains the form factor of each hemi-cube pixel [CG85], A is a vector with the area of all the scene patches, and s is a vector that contains the luminance ($lm/sr/m^2$) of each sky tile. $\mathbf{B}_c$ is a $n_c \times \bar{s}$ matrix where each column contains the radiosity (B_c) exterior vector related to a sky tile (Sec. 3.2).

$$\mathbf{G}_s(i,j) = \sum_{k=1}^{\bar{s}} \underbrace{\left(\frac{A(j)}{A(i)} \sum_{\substack{u,v| \\ \mathbf{H}_j^I(u,v)=i}} \pi\Delta\mathbf{F}(u,v)\mathbf{B}_c(\mathbf{H}_j^E(u,v),k) \right)}_{\mathbf{L}(i,j,k)} s(k) \tag{5}$$

Figs. 2(b)-(d) show that the inner elements of Eq. 5 allows to know the exterior light arriving to pinhole j. The light is projected from the pinholes j that can belong to the opening (Fig. 2(f)) into the internal model (Fig. 2(g)). The pinhole projection is obtained by rotating 180^o the image in Fig. 2(d). Finally, Fig. 2(h) shows the values of $\mathbf{G}(i,j)$ associated to each interior patch i and a given pinhole j.

Eq. 5 can be simplified by grouping most of its components in a tensor (a 3D matrix) $\mathbf{L}$ of dimension $n_o \times \bar{w} \times \bar{s}$:

$$\mathbf{G}_s = \mathbf{L} \times_3 s \tag{6}$$

The cells of $\mathbf{L}$ are independent of s, therefore they can be calculated only once for all the sky configurations. The term $\times_i$ specifies a tensor times vector product along the i^{th} dimension of the tensor.

Combining Eqs. 4 and 6 it is possible to find a new expression for $\mathbf{N}_s$. As stated above, $\mathbf{Q}$ (see Eq. 7) is a $n_o \times w \times \bar{s}$ tensor invariant to the sky configuration.

$$\begin{aligned} \mathbf{N}_s &= (\mathbf{I}_o - \mathbf{R}_o\mathbf{F}_o)^{-1}(\mathbf{L} \times_3 s) \\ &= \underbrace{((\mathbf{I}_o - \mathbf{R}_o\mathbf{F}_o)^{-1} \times_1 \mathbf{L})}_{\mathbf{Q}} \times_3 s = \mathbf{Q} \times_3 s \end{aligned} \tag{7}$$

$\mathbf{N}_s(P,:) = \mathbf{Q}(P,:,:) \times_3 s$ contains all relevant information for a given set of sensors P and a sky configuration s. Therefore, given a climate-based data with thousands of skies $S=\{s_1, ..., s_{\bar{S}}\}$ and an opening W, Eq. 8 allows to calculate the vector I_S of dimension $\bar{S}\bar{P}$ that contains the illuminance in all sensors P for all the skies in S.

$$I_S = \mathbf{N}_{S,P} W = \begin{pmatrix} \mathbf{N}_{s_1}(P,:) \\ \vdots \\ \mathbf{N}_{s_{\bar{S}}}(P,:) \end{pmatrix} W = \begin{pmatrix} \mathbf{Q}(P,:,:) \times_3 s_1 \\ \vdots \\ \mathbf{Q}(P,:,:) \times_3 s_{\bar{S}} \end{pmatrix} W \tag{8}$$

I_S is used to calculate the UDI hours of the interior model [FBB16].

3.4. Opening shape optimization

We use a rectangle-based shape in order to define the optimal opening. We can use one or more rectangles that are built over a wall previously set to have openings installed. Each rectangle is defined

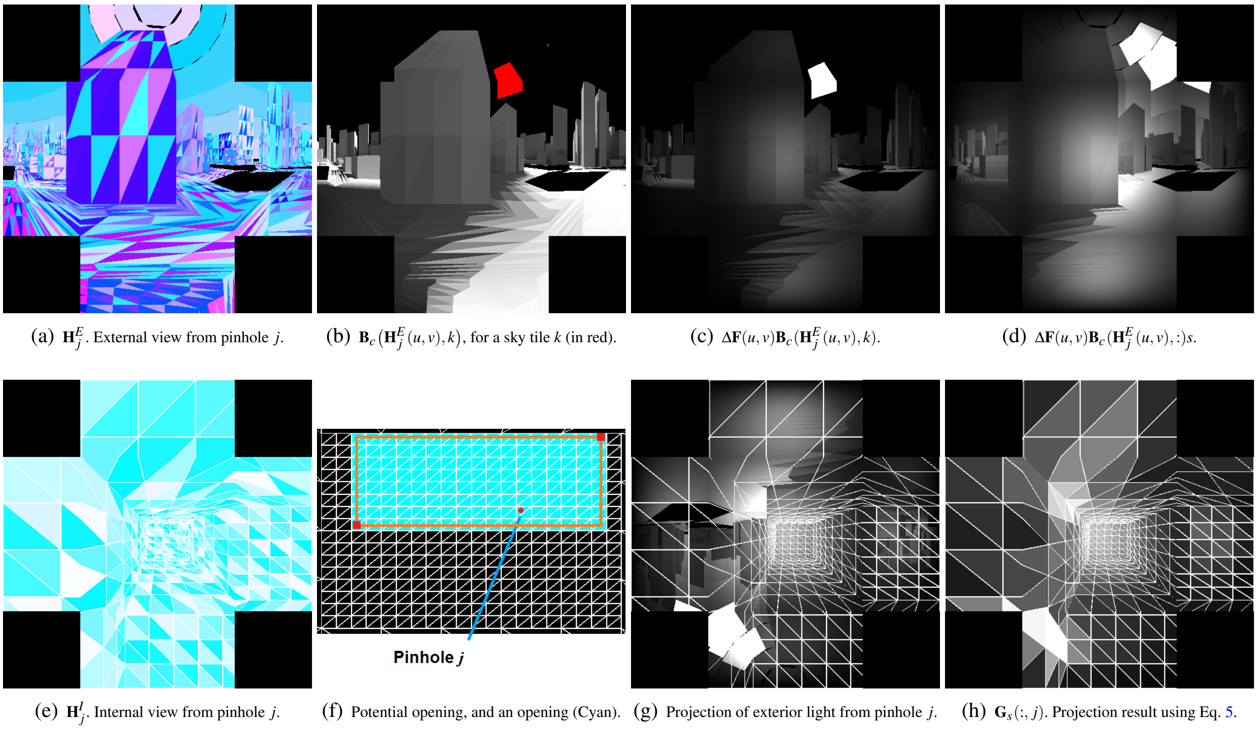

(a) $\mathbf{H}_j^E$. External view from pinhole j.
(b) $\mathbf{B}_c(\mathbf{H}_j^E(u,v),k)$, for a sky tile k (in red).
(c) $\Delta\mathbf{F}(u,v)\mathbf{B}_c(\mathbf{H}_j^E(u,v),k)$.
(d) $\Delta\mathbf{F}(u,v)\mathbf{B}_c(\mathbf{H}_j^E(u,v),:)s$.
(e) $\mathbf{H}_j^I$. Internal view from pinhole j.
(f) Potential opening, and an opening (Cyan).
(g) Projection of exterior light from pinhole j.
(h) $\mathbf{G}_s(:,j)$. Projection result using Eq. 5.

Figure 2: *Components of Eq. 5: (a) Color code of external patches in a hemi-cube view. (b) External view when the emitter is only one sky tile. (c) The image (b) is ponderated by* $\Delta\mathbf{F}$. *(d) External view for a particular sky configuration s. (e) Color code of the interior "office" patches, as it is seen from patch j. (f) Potencial opening patches* (640)*, and a particular window configuration. (g) Projection of exterior light from pinhole j onto the interior geometry. (h) Result of Eq. 5 applied to all interior patches and pinhole j.*

by two opposite corners, and all the patches elements that fall inside a rectangle partially or totally, are considered to be part of the opening (see Fig. 2(f)). Each corner of a rectangle opening can be represented as a 2D vector. Working with corner bounds has the advantage of reducing the number of variables to iterate in the optimization. Also, it ensures the existence of large sets of connected patches. We associate each patch of those surfaces to a cell in vector W. Then, the value of each W cell is 1 when its corresponding patch is partially or totally inside the rectangle, and 0 otherwise. After that, Eq. 8 allows to find the UDI related to the opening [FBB16].

For the optimization process, we use the Variable Neighborhood Search (VNS) method [HM01] with the goal of maximizing the daylight availability. VNS is a global optimization metaheuristic. It starts with a random configuration of rectangles (openings) which evolves to the solution. This process implies thousands of evaluations of Eq. 8, one for each opening configuration tested. More details of the process are explained in [FBB16].

4. Results

In this section we present a set of experiments in order to illustrate the use of the method. Figs. 3 and 4 show the urban and office models used, respectively, whereas the main results are summarized in Table 1. The simulations were conducted on a desktop computer, with Intel quad-core i7 processor, 8 Gbytes RAM, and a NVIDIA GeForce-780 GPU processor. The code was implemented mainly in MATLAB [MAT10], using C++, OpenGL, and CUDA [KH10] for the computation of $\mathbf{F}_c$.

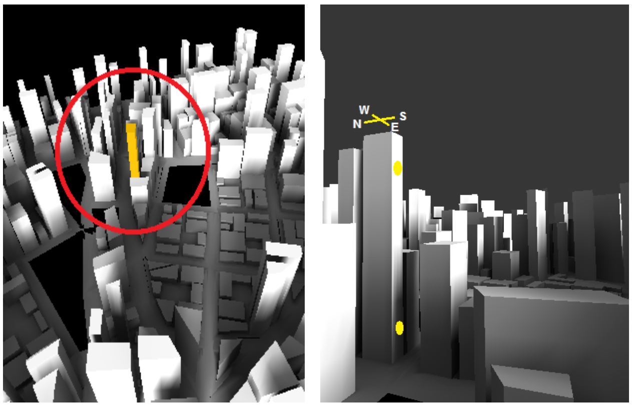

Figure 3: *Urban model and the selected building. The yellow points at the facade show the location of the up and bottom south views.*

The urban model (Fig. 3) is composed by 142352 patches, where the reflection index of all the surfaces is set to 0.3. The climate-based data corresponds to Gatwick, London-UK. It is derived from the direct normal and diffuse horizontal irradiation data, extracted from Test Reference Year data [EER16]. For the interior model, we take the same office room as in [NM05] (Fig. 4). The office is a box composed by 1260 patches, where 640 of them correspond to the potential opening surface (Figs. 2(e) and (f)), located in one of its walls. This surface can cover an entire wall, except for a lower section of 0.75m high. The window glass has a transmittance of 0.76, whereas the reflectivities of the walls, ceiling, and floor are 0.7, 0.8, and 0.2, respectively. For our tests, we compute the optimal window shape for the office room at different heights (up and bottom) of the same facade of the building and also for different orientations (North and South). See Fig. 3.

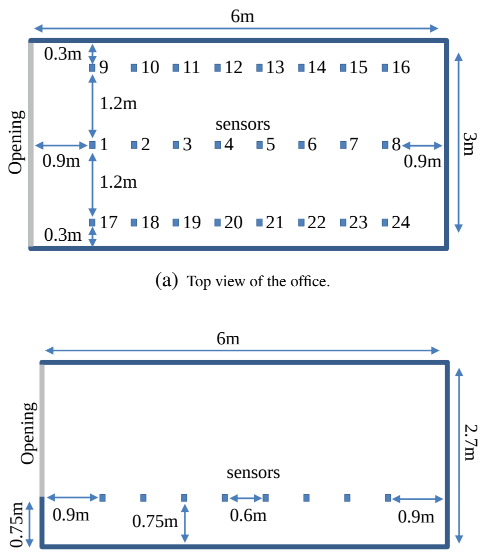

(a) Top view of the office.

(b) Lateral view.

Figure 4: *Office model with 24 sensors, distributed in three rows.*

The calculation of $\mathbf{F}_c$ takes about 600s. The matrix $\mathbf{F}_c$ is sparse, with only 0.64% of non-zero elements. Its sparseness allows to store it in main memory, with a size of almost 2 GBytes. The calculation of the external radiosity (matrix $\mathbf{B}_c$ in Eq. 5) considering each of the 145 sky tiles as emitters takes about 140s after 5 iterations of Eq. 2. Moreover, the maximum number of iterations for the test case is 42, because $||\mathbf{B}_c^{(42)} - \mathbf{B}_c^{(41)}||/||\mathbf{B}_c^{(41)}||$ is lesser than the machine epsilon. This last process takes about 1000s to finish.

Table 1 summarizes the main results. In column 1 from left to right, the external hemi-cube views for up-south, bottom-south and up-north locations are shown. The variation of the external views can be appreciated, as well as the obstruction of the sky by the environment. The UDI hours shown in these figures correspond to the office when the opening includes all the 640 potential patches.

Columns 2 to 4 in Table 1 show optimal window shapes after running 20000 iterations of the VNS metaheuristic. Each calculation of $N_{S,P}$ takes about 20 minutes, and each optimization process takes about 30 minutes. These optimal openings maximize the UDI hours for different daylighting conditions, opening constraints, and locations. We tested the method for one rectangular window, where the ratio between the height and width is between 3 and $1/3$ (Columns 2 and 3), and with openings composed of two rectangles with no ratio restriction (Column 4)

Column 2 shows the optimal openings ignoring the ERC component, that is, the sensors only receive SC and IRC components of daylight. For comparison purposes, after the optimal shapes are found, the UDI hours are then computed for the resulting openings considering all light components.

Column 3 shows the optimal solutions for the same case as above, but now considering the ERC component. This component was calculated using both 5 and 42 light bounces, but in both cases the UDI hours were the same, meaning that only the first bounces of light are sufficient in most cases. We can observe that when the sky view is occluded by buildings, then the UDI hours vary greatly between columns 2 and 3. Then, we conclude that it is very important to consider reflections in urban environments.

Finally, in Column 4 another optimum solution is shown for each building location. Here it is allowed to have two rectangular window that can overlap each other. Also, there is no height-width constraints. In this scenario, the gain increased up-to 302% compared to the completely open window. The gain is also significant in comparison to the 3^{rd} column. Therefore, when the set of possible solutions is much wider, it is possible to obtain a significant increase in the amount of UDI hours.

5. Conclusions and Future Work

We presented an opening optimization method using climate-based data capable of dealing with an urban context including all components. The correct treatment of the external reflected component is a major contribution of our work. We show, through different window shape results, the importance of accurately computing the urban influence in daylighting assessment. The other important contribution is that our method can deal with such a huge-data problem efficiently in processing time and memory.

Further work includes the experimental evaluation of the process and results in real urban environments. Another important aspect to consider is related to the number of iterations of Eq. 2, suited for practical purposes. The proposed technique can influence the process of building design, as well as the definition of city regulations. To include thermal aspects into the proposal, we should consider the addition of the heat equation.

Acknowledgments

The work was partially supported by FSE_1_2014_1_102344 project from Agencia Nacional de Investigación e Innovación (ANII, Uruguay) and TIN2014-52211-C2-2-R project from Ministerio de Economía y Competitividad, Spain.

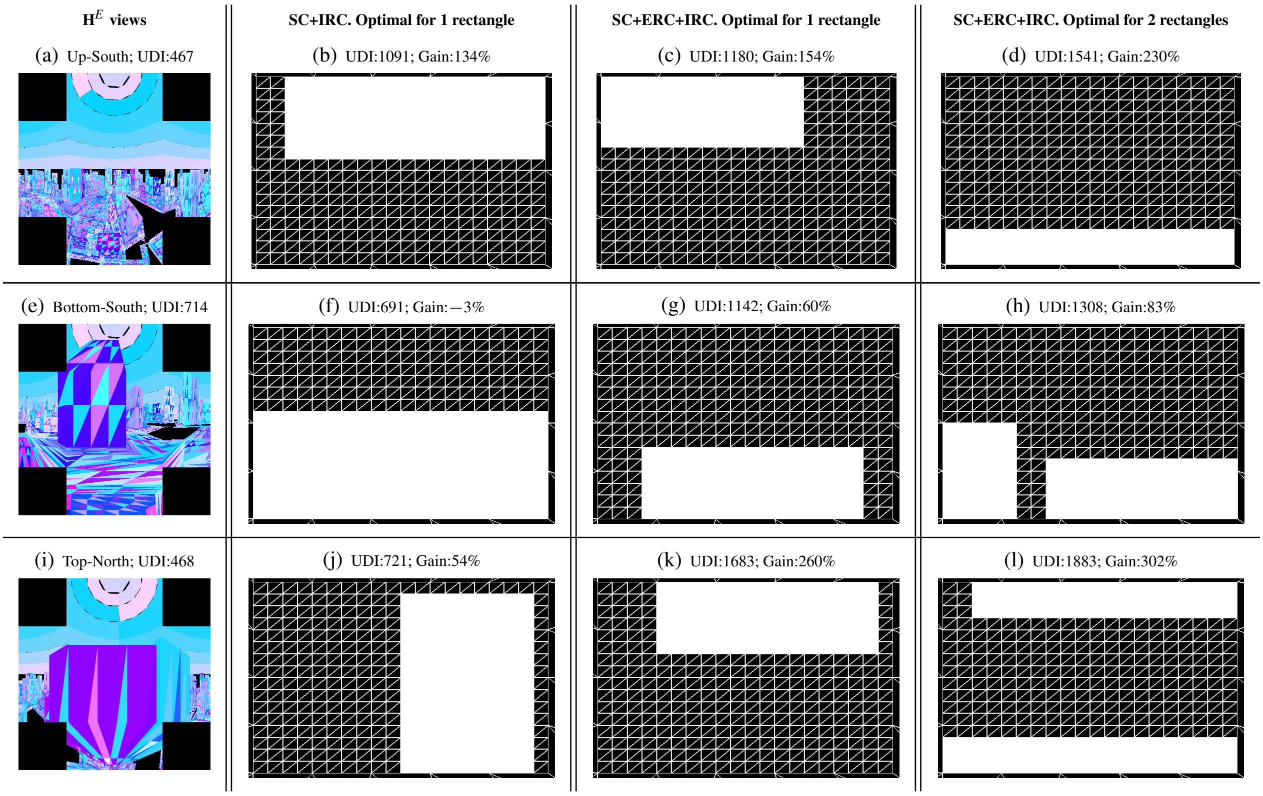
$\mathbf{H}^E$ views
SC+IRC. Optimal for 1 rectangle
SC+ERC+IRC. Optimal for 1 rectangle
SC+ERC+IRC. Optimal for 2 rectangles

(a) Up-South; UDI:467

(b) UDI:1091; Gain:134%

(c) UDI:1180; Gain:154%

(d) UDI:1541; Gain:230%

(e) Bottom-South; UDI:714

(f) UDI:691; Gain:−3%

(g) UDI:1142; Gain:60%

(h) UDI:1308; Gain:83%

(i) Top-North; UDI:468

(j) UDI:721; Gain:54%

(k) UDI:1683; Gain:260%

(l) UDI:1883; Gain:302%

Table 1: $\mathbf{H}^E$ *views for different building locations and their UDI hours when the window is completely open (Col,* 1*). Rows show optimal openings for each location. The gains shown are calculated comparing with the completely open window.*

References

[AFBB16] Aguerre J., Fernández E., Besuievsky G., Beckers B.: Sparse matrix solution for computing urban radiation exchange. In *Proceedings of First International Conference on Urban Physics (FICUP)* (September 2016). 1, 2

[Aut14] Autodesk Inc: Autodesk ecotect analysis, 2014. (Sep 2014). 2

[BT09] Besuievsky G., Tourre V.: A daylight simulation method for inverse opening design in buildings. In *Proceedings of the IV Iberoamerican Symposium in Computer Graphics* (June 2009), Sociedad Venezolana de Computación Gráfica, DJ Editores, C.A., pp. 29–46. 2

[CG85] Cohen M. F., Greenberg D. P.: The hemi-cube: a radiosity solution for complex environments. *SIGGRAPH Comput. Graph. 19*, 3 (July 1985), 31–40. 3

[CSFN11] Cassol F., Schneider P. S., França F. H., Neto A. J. S.: Multi-objective optimization as a new approach to illumination design of interior spaces. *Building and Environment 46*, 2 (2011), 331–338. 1

[CWH93] Cohen M. F., Wallace J., Hanrahan P.: *Radiosity and Realistic Image Synthesis*. Academic Press Professional, Inc., San Diego, CA, USA, 1993. 2

[EER16] EERE: Weather data downloaded from the website: http://energy.gov/eere/office-energy-efficiency-renewable-energy, visited in, July 2016. 5

[FB12] Fernández E., Besuievsky G.: Inverse lighting design for interior buildings integrating natural and artificial sources. *Computers & Graphics 36*, 8 (2012), 1096–1108. 1, 2, 3

[FB14] Fernández E., Besuievsky G.: Efficient inverse lighting: A statistical approach. *Automation in Construction 37*, Complete (2014), 48–57. 2

[FB15] Fernández E., Besuievsky G.: Inverse opening design with anisotropic lighting incidence. *Computers & Graphics 47* (2015), 113 – 122. 1, 2, 3

[FBB16] Fernández E., Beckers B., Besuievsky G.: A fast daylighting method to optimize opening configurations in building design. *Energy and Buildings 125* (2016), 205 – 218. 1, 2, 3, 4

[FOB15] Futrell B. J., Ozelkan E. C., Brentrup D.: Optimizing complex building design for annual daylighting performance and evaluation of optimization algorithms. *Energy and Buildings 92* (2015), 234 – 245. 2

[HM01] Hansen P., Mladenovic N.: Variable neighborhood search: Principles and applications. *European Journal of Operational Research 130*, 3 (May 2001), 449–467. 4

[HW15] Hiyama K., Wen L.: Rapid response surface creation method to optimize window geometry using dynamic daylighting simulation and energy simulation. *Energy and Buildings 107* (2015), 417 – 423. 2

[KH10] Kirk D. B., Hwu W.-M. W.: *Programming Massively Parallel Processors: A Hands-on Approach*, 1st ed. Morgan Kaufmann Publishers Inc., San Francisco, CA, USA, 2010. 4

[MAT10] MATLAB: *version 7.10*. The MathWorks Inc., Natick, Massachusetts, 2010. 4

[ML13] McNeil A., Lee E.: A validation of the radiance three-phase simulation method for modelling annual daylight performance of optically complex fenestration systems. *Journal of Building Performance Simulation 6*, 1 (2013), 24–37. 1

[NM05] Nabil A., Mardaljevic J.: Useful daylight illuminance: a new paradigm for assessing daylight in buildings. *Lighting Research and Technology 37*, 1 (January 2005), 41–59. 1, 5

[Rei14] Reinhart C.: *Daylighting Handbook: fundamentals, designing with the sun*. No. v. 1 in Daylighting Handbook. Christoph Reinhart, 2014. 2

[RMR06] Reinhart C. F., Mardaljevic J., Rogers Z.: Dynamic daylight performance metrics for sustainable building design. *LEUKOS 3*, 1 (2006), 7–31. 1

[TMH08] Tourre V., Martin J.-Y., Hégron G.: An inverse daylighting model for CAAD. In *SCCG '08: Proceedings of the 24th Spring Conference on Computer Graphics* (Comenius University, Bratislava, 2008), pp. 95–102. 2

[TW83] Tregenza P., Waters I.: Daylight coefficients. *Lighting Research and Technology 15*, 2 (1983), 65–71. 1, 2

[WML*11] Ward G., Mistrick R., Lee E. S., McNeil A., Jonsson J.: Simulating the daylight performance of complex fenestration systems using bidirectional scattering distribution functions within radiance. *LEUKOS 7*, 4 (2011), 241–261. 1